HHS Public Access
Author manuscript
Cell Rep. Author manuscript; available in PMC 2016 September 11.

Published in final edited form as:
Cell Rep. 2015 March 17; 10(10): 1655–1664. doi:10.1016/j.celrep.2015.02.037.

A lupus-associated Mac-1 variant has defects in integrin allostery and interaction with ligands under force

F Rosetti[1,2,*], **Y Chen**[3,4,*], **M Sen**[5], **E Thayer**[1], **V Azcutia**[1], **JM Herter**[1], **FW Luscinskas**[1], **X Cullere**[1], **C Zhu**[3,4,6,#], and **TN Mayadas**[1,#]

[1]Department of Pathology, Center for Excellence in Vascular Biology, Brigham and Women's Hospital and Harvard Medical School, Boston, MA 02115

[2]Immunology Graduate Program, Division of Medical Sciences, Harvard Graduate School of Arts and Sciences at Harvard Medical School, Boston, MA 02115

[3]Woodruff School of Mechanical Engineering, Georgia Institute of Technology, Atlanta, GA 30332

[4]Institute for Bioengineering and Bioscience, Georgia Institute of Technology, Atlanta, GA 30332

[5]Program in Cellular and Molecular Medicine, Immune Disease Institute, Children's Hospital, Harvard Medical School, Boston, MA 02115

[6]Coulter Department of Biomedical Engineering, Georgia Institute of Technology, Atlanta, GA 30332

SUMMARY

Leukocyte CD18 integrins increase affinity for ligand via transmission of allosteric signals to and from their ligand binding αI-domain. Mechanical forces induce allosteric changes that paradoxically slow dissociation by increasing integrin/ligand bond lifetimes, referred to as catch bonds. Like LFA-1, Mac-1 (ITGAM) forms catch bonds with its ligands. However, the Mac-1 rs1143679 (R77H) variant, located in the β-propeller domain and significantly associated with systemic lupus erythematosus risk, exhibits a marked impairment in 2D ligand affinity and affinity maturation under mechanical force. Targeted mutations and activating antibodies reveal that the failure in Mac-1 R77H allostery is rescued by induction of cytoplasmic tail separation and full integrin extension. These findings demonstrate roles for R77, and the β-propeller in which it resides, in force-induced allostery relay and integrin bond stabilization, suggesting that these

Contact for corresponding authors: Tanya N. Mayadas: tmayadas@rics.bwh.harvard.edu, Cheng Zhu: cheng.zhu@bme.gatech.edu.
*These authors contributed equally to this work.
#Co-corresponding authors

AUTHOR CONTRIBUTIONS

Experiments were performed and analyzed by FR, YC, ET, VA, JH. FR generated the mutants and cell lines, conducted experiments under static and flow conditions and the FACs analysis. YC generated and analyzed the BFP data. MS constructed the Mac-1 structure and XC aided in generating mutants. WL gave advice for flow assays. The study was designed and the manuscript written by FR, YC, MS, CZ and TM.

The authors have no conflicts of interest to disclose.

defects may have pathological consequences as the Mac-1 R77H variant associates with increased lupus susceptibility.

INTRODUCTION

Leukocyte integrins, composed of a unique α complexed to a common β_2 subunit, are a major family of adhesive receptors. The regulation of their affinity for ligands is key to cell adhesion and occurs through structural changes in their extracellular domains. These allosteric changes occur upon cell activation by chemokines, ligand binding, and cytoplasmic regulators (Carman and Springer, 2003), and can also be induced by mechanical forces that prolong the lifetime of receptor-ligand bonds (Chen et al., 2010; Choi et al., 2014; Fiore et al., 2014; Kong et al., 2009), a counter-intuitive phenomenon called catch bonds. Catch bonds may allow leukocytes to roll stably and adhere firmly to the vessel wall, and to migrate and form an immunological synapse with antigen presenting cells. Humans lacking β_2 integrins (Leukocyte Adhesion Deficiency I, LADI) or intracellular molecules required for integrin activation (LADIII) exhibit significant defects in host defense, demonstrating the importance of integrins and their activation in immune cell function (Abram and Lowell, 2009). However, to date, there is no evidence that alterations in integrin allostery or catch bonds have pathological consequences in humans.

In two independent mouse models of systemic lupus erythematosus (SLE), a multi-organ autoimmune disease (Tsokos, 2011), Mac-1 ($\alpha_M\beta_2$) deficiency increases susceptibility to developing nephritis (Kevil et al., 2004; Rosetti et al., 2012). In humans, genome wide association studies identified variants of the *ITGAM* gene, which encodes the α_M chain, as risk factors for SLE (Hom et al., 2008; Yu et al., 2012). Despite the identification of several Mac-1 single nucleotide polymorphisms (SNP), a strong risk effect was mapped to rs1143679 that results in the substitution of Arginine for a Histidine at position 77 (R77H) (Han et al., 2009). Although the R77H variant compromises Mac-1 adhesive functions, the extent of which varies between studies (Fagerholm et al., 2013; Zhou et al., 2013), the molecular mechanism for how this variant, located in the β-propeller outside of the ligand binding αI-domain, affects ligand binding is unclear. Ligand binding by Mac-1 is contained within the αI-domain, inserted in the β-propeller domain of the α-subunit. The homologous αI and the β_2 subunit βI-domains bind Mg^{2+} at their Metal Ion-Dependent Adhesion Sites (MIDAS), which coordinates an invariant Glu or Asp shared by integrin ligands. Integrin activation leads to cytoplasmic α/β tail separation and integrin extension. The extension facilitates the sequential outward movement of the hybrid domain, the downward shift of the βI α7-helix and the opening of the βI-domain, which enhances βI-MIDAS binding to the C-terminal αI domain α7-helix, which serves as an internal ligand. Internal ligand binding leads to a downward shift of the αI α7-helix and thus activation of the αI-MIDAS for high-affinity binding of the external ligand (Carman and Springer, 2003).

Here, we demonstrate that α_M^{R77H} reduces 2D ligand binding affinity and force-regulated dissociation of receptor-ligand bonds (catch-bonds). The latter is rescued by mutations and an activating antibody distal to R77H that are documented to induce integrin allosteric changes, indicating that R77H regulates integrin allostery needed to prolong the lifetime of adhesive bonds under shear flow. A reduction in Mac-1's binding affinity and bond stability may impact the immunomodulatory function of Mac-1 and thus contribute to lupus susceptibility.

RESULTS

Neutrophils expressing the Mac-1 R77H variant have defects in neutrophil adhesion under hydrodynamic forces

The crystal structure of the sister integrin $\alpha\beta_2$ (Sen et al., 2013), which is 60% identical to Mac- 1 (Yu et al., 2012), was used to model Mac-1. Domains were further adjusted using the open headpiece of $\alpha^{IIb}\beta^3$ integrin (Xiao et al., 2004) to make an extended-open Mac-1 integrin (Figure 1A). The R77H mutation exists in the outer rim of the β-propeller, in close proximity to the αI-domain. The schematic also contains the location of binding sites of activation reporter, functional blocking and control antibodies used in our study (Figure 1A).

To assess the functional repercussions of R77H we evaluated human neutrophils homozygous for the risk (R77H; rs1143679) or the non-risk variant. Surface expression of Mac-1 (Figure 1B), exposure of the α_M activation reporter epitope CBRM1/5 (Figure 1C), neutrophil activation markers, and other surface molecules (e.g. $\alpha\beta_2$ and CD32) (Figure S1A) was similar upon stimulation with the chemokine fMLP. Thus, R77H has no effect on expression and activation of Mac-1 on neutrophils, as previously reported (Zhou et al., 2013). Adhesion assays on complement iC3b coated surfaces were done under static or shear flow conditions following fMLP treatment. Neutrophil binding was significantly reduced by Mac-1 blocking antibodies (Table S1), and neutrophils with the R77H variant had no defects in binding under static conditions (Figure 1D), spreading (Figure 1E), or phagocytosis (data not shown). However, they exhibited a significant decrease in ligand binding under shear flow (Figure 1F). They also displayed a trend towards reduced velocity during random migration induced by shear force (Figure 1G), a Mac-1 dependent function (Phillipson et al., 2006) that, like adhesion under shear flow, requires optimal integrin on- and off-rates. These results were recapitulated with neutrophils from healthy volunteers treated with functional blocking antibodies to the β-propeller domain in which R77H resides: CBRN1/6, 3/4 and 1/32 partially affected adhesion under static conditions but abrogated ligand binding under shear flow while CBRM1/20, another β-propeller antibody and a control-binding antibody, CBR LFA1/7, had no effect (Figure 1H,I and Table S1). All antibodies bound Mac-1 similarly (Figure S1B). iC3b may also have binding sites in the β-propeller (Yalamanchili et al., 2000). However, β-propeller blockade prevented binding to both ICAM-1 and iC3b under flow (Table S1) suggesting that our results are not due solely to direct inhibition of iC3b binding to the β-propeller. Finally, β-propeller inhibition hindered the migration velocity of neutrophils as did an antibody to the αI-domain (Figure 1J).

Residue R77 and the β-propeller are required for mechanical force-induced adhesion in K562 cells expressing Mac-1

We found that 90% of the neutrophil samples homozygous for the R77H were also homozygous for two other SLE-associated SNPs, rs1143683 and rs1143678 present in the

Calf-1 and cytoplasmic domain of *ITGAM* respectively, as reported by others (Zhou et al., 2013). To assess the R77H-specific contribution we evaluated the human leukemic cell line K562 stably expressing similar levels of $\alpha_M^{WT}\beta_2$ or $\alpha_M^{R77H}\beta_2$ (Figure S2A) and K562 cells alone following their treatment with Mg^{2+}/EGTA or Mn^{2+} to directly activate integrins (Xiao et al., 2004). Mac-1 activation, examined with activation-reporter antibodies was similar in both groups (Figure S2B). Under static conditions, Mg^{2+}/EGTA activated α_M^{R77H} cells had a significant defect in binding to iC3b-surfaces but Mn^{2+} treated α_M^{WT} and α_M^{R77H} cells bound equivalently (Figure 2A), the latter being consistent with the comparable binding capacity observed in fMLP stimulated neutrophils from risk and non-risk variant (Figure 1D). The differential requirement for R77H in the presence of Mn^{2+} versus Mg^{2+}/EGTA in static assays may reflect the occupation of all three βI-domain metal sites by Mn^{2+} that, coupled with high ligand density, maximizes the on-rate and integrin avidity and thus bypasses the need for R77. On the other hand, Mg^{2+}/EGTA blocks the occupancy and thus the negative regulatory role of Ca^{2+} at the ADMIDAS (Xiong et al., 2003), which results in less stable internal ligand binding and requires R77 for full integrin activation. Under shear flow, R77H had a defect in binding ICAM-1 in the presence of Mg^{2+}/EGTA at shear stresses from 0.19–0.42 dynes/cm^2 with the most significant difference observed at 0.38 dynes/cm^2 (Figure S2C). Further analysis at this shear stress revealed impaired binding of α_M^{R77H} cells to iC3b or ICAM-1 in the presence of either Mn^{2+} or Mg^{2+}/EGTA (Figure 2B). In addition, while β-propeller antibodies only partially affected adhesion under static conditions, they significantly abrogated ligand binding under shear flow (Figures 2C,D, S1C and Table S1). The similarity of results with human neutrophils suggests that R77H in the β-propeller is primarily responsible for the observed adhesion defects in human neutrophils.

Separation of the α and β subunit cytoplasmic tails but not βI-domain activation rescues the Mac-1-R77H binding defect under flow

Mutations in the βI-domain of $\alpha_X\beta_2$ that increase its affinity for the αI α7-helix internal ligand result in a greater population of αI-domain in the open conformation, and thus stabilize $\alpha_X\beta_2$ in an extended conformation with an open headpiece (Sen et al., 2013). K562 cells expressing α_M^{WT} or α_M^{R77H} coupled to β_2 subunit with or without activating mutations V124A (Figure S3A) or L132A (data not shown) were tested in adhesion assays to determine their ability to restore R77H binding defects. Both $\alpha_M^{WT}\beta_2^{V124A}$ and $\alpha_M^{R77H}\beta_2^{V124A}$ adopted an extended-open conformation in the absence of activating cations (Figure S3B), as predicted (Sen et al., 2013). However, α_M^{R77H} with β_2^{V124A} (Figure 2E) or β_2^{L132A} (data not shown) remained impaired in ligand binding under flow. The small molecule Leukadherin-1 (LA-1) binds and activates the αI-domain without inducing global conformational changes (Faridi et al., 2013). While LA-1 pretreatment enhanced adhesion of α_M^{WT} expressing cells (data not shown) as described (Faridi et al., 2013), it did not rescue the ability of α_M^{R77H} to bind iC3b under flow (Figure 2F). Thus, neither an open, permissive βI-domain nor the direct activation of the αI-domain rescues R77H.

Mn^{2+} and chemokine treatments favor integrin extension but do not result in cytoplasmic tail separation (Kim et al., 2003; O'Brien et al., 2012). We exploited the CBR LFA1/2 antibody that binds to the membrane proximal I-EGF-3 of the β_2 subunit (Lu et al., 2001) (see Figure

1A) and induces integrin extension (Petruzzelli et al., 1995) and cytoplasmic tail separation in both $\alpha_M\beta_2$ (Lefort et al., 2009) and $\alpha_L\beta_2$ (Kim et al., 2003). CBR LFA1/2 rescued the binding defect of α_M^{R77H} cells (Figure 2G). To validate this conclusion, we deleted the α_M cytoplasmic tail and therefore the GFFKR (ΔGFFKR) sequence, the mutation of which has been shown to result in tail separation and a fully extended, active integrin in the absence of activating cations (Kanse et al., 2004; Kim et al., 2003; Lu and Springer, 1997). Cells expressing $\alpha_M^{R77H\Delta GFFKR}$ resumed the ability to bind ligand under shear flow (Figure 2H). Unlike $\alpha_L\beta_2$ (Lu and Springer, 1997), ΔGFFKR in $\alpha_M\beta_2$ did not lead to constitutive extension and headpiece opening but Mg^{2+}/EGTA or Mn^{2+} induced similar conformational changes in $\alpha_M^{R77H\Delta GFFKR}$ and $\alpha_M^{WT\Delta GFFKR}$ (Figure S3C,D). Thus, forcing the tail and lower leg separation of the α and β subunits, using both antibody and genetic approaches, restored adhesion in R77H cells.

R77H reduces the binding affinity of Mac-1 at zero-force by decreasing its on-rate

To understand the effects of R77H on Mac-1's ligand binding kinetics, we used a biomembrane force probe (BFP) (Figure 3A) to measure single-bond interactions between Mac-1 expressing cells and ICAM-1 bearing beads in the presence of Mg^{2+}/EGTA (Figure 3B). We analyzed the absence (Figure 3C, cyan) or presence (Figure 3C, magenta) of binding after a contact of given duration to obtain adhesion frequency; and when binding occurred, the lifetime of (most likely) a single bond under a desired force (Figure 3C). The adhesion frequencies of α_M^{WT} cells (magenta circle) with ICAM-1 were higher than those of α_M^{R77H} (cyan square) over a range of contact times, even though the α_M^{WT} cells had lower Mac-1 surface expression (Figure 3D). An anti-αI domain blocking antibody CBRM1/29 abrogated adhesion, and streptavidin-coated beads blocked with BSA also showed rare adhesion events, confirming Mac-1 and ICAM-1 specificity (Figure 3D). The adhesion frequency versus contact time data were fit to Equation 1 in Materials and Methods along with the site densities m_r and m_l to evaluate the effective 2D affinities (Figure 3E) and stress-free off-rates (Figure 3F). R77H significantly reduced Mac-1 binding affinity but not the off-rate (Figure 4E,F). As affinity is the ratio of on- to off-rate, this indicates that R77H reduced the binding affinity of Mac-1 for ICAM-1 via reducing its on-rate. The lower affinity and on-rate of α_M^{R77H} versus α_M^{WT} at zero force provides a plausible explanation for the defect in static adhesion of α_M^{R77H} cells in the presence of Mg^{2+}/EGTA (Figure 2A).

Mac-1 R77H suppresses allosteric catch bonds

The mechanical regulation of Mac-1/ICAM-1 dissociation was quantified by the BFP. Zero-force bond lifetimes measured by thermal fluctuation were short and distributed as straight lines in the semi-log survival frequency versus bond lifetime plots for both α_M^{WT} (Figure 3G) and α_M^{R77H} (Figure 3I). Their calculated off-rates are not significantly different (Figure 3G, I) and comparable to the values obtained in the adhesion frequency assay (Figure 3F).

By comparison, lifetimes of $\alpha_M\beta_2$/ICAM-1 bonds at low forces were distributed as two line segments in these semi-log plots, revealing two subpopulations of bonds (Figure 3G). The first subpopulation was fast dissociating with off-rates comparable to the bonds at zero-force. The second subpopulation has much slower dissociating rates, which equal the negative slopes of the second line segments (Figure 3G). For α_M^{R77H} (Figures 3I,J), the slopes of the second line segments are much steeper (i.e. higher off-rates) compared to α_M^{WT} (Figure 3G,H) at matched forces (≥5pN). Similar force induction of slow dissociating subpopulation of bonds has been observed for $\alpha_L\beta_2$/ICAM-1, which results in catch bonds (Chen et al., 2010; Xiang et al., 2011).

To examine if Mac-1 forms catch bonds with ICAM-1, bond lifetimes were plotted against force. For α_M^{WT}, as force increased, the lifetime first increased and reached the maximum at 12pN, then decreased, exhibiting a biphasic transition from catch to slip (Figure 3K). In comparison, the catch-slip trend of α_M^{R77H} was suppressed; the sharp summit in α_M^{WT} transformed into a relatively flat plateau with a one-fold drop in amplitude, a leftward shift and a marked shrinking of the catch regime to ≤5pN, and a downward shift at the higher forces slip regime (Figure 3K). At ~12pN where α_M^{WT} reached the highest lifetime of 4s, the α_M^{R77H} bond with ICAM-1 was 3-fold shorter-lived (~1s). Catch-bonds were attributed to $\alpha_M\beta_2$/ICAM-1 interactions as the rare adhesions of streptavidin-coated beads to α_M^{WT} cells in the presence of BSA alone showed negligible lifetimes under all forces (Figure S4A). As BSA can under some conditions bind Mac-1 (Yalamanchili et al., 2000), PVP was used alternatively to block non-specific binding, which yielded similar results to BSA (Figure S4A), again suggesting that the short-lived bonds (Figures 3G–J) do not stem from potential Mac-1/BSA interactions.

Therefore, R77H suppresses catch bonds, thus impairing the ability of cells to sustain their association with ICAM-1 under forces, but does not impact bond stability under force-free conditions. This is concordant with the adhesion assays, which show that R77H primarily impairs ligand binding under flow.

Rescue of catch bonds in Mac-1 R77H by activating antibody CBR LFA1/2

CBR LFA1/2 treatment resulted in indistinguishable adhesion frequency versus contact time curves for α_M^{WT} and α_M^{R77H} (Figure S4B), with increased 2D affinities and reduced zero-force off-rates (Figure 3E,F) for both forms of Mac-1. Significantly, this antibody induced sizable subpopulations of slow dissociating bonds with very long lifetimes over a wide range of forces for both α_M^{WT} (Figure S4E,F) and α_M^{R77H} (Figure S4G,H). This rendered an enhanced catch bond for α_M^{WT} with longer lifetimes in all forces than without the antibody (Figure 3L). The CBR LFA1/2 also increased the α_M^{R77H} bond lifetime, and rescued the sharp catch-slip biphasic trend (Figure 3L). Notably, the two lifetime curves of α_M^{WT} and α_M^{R77H} overlapped under all forces, indicating the impairment of the mutation on off-rate was completely overcome by CBR LFA1/2. The control antibody CBR LFA1/7 confirmed the specificity of the activating effect of CBR LFA1/2 (Figure 3L).

Cytoplasmic tail separation rescues the catch bond in R77H, while activation of the βI domain has only a partial effect

GFFKR deletion increased the 2D affinity and reduced the zero-force off rate for α_M^{WT} but not α_M^{R77H} (Figures 3E,F and S4C). Nonetheless, $\alpha_M^{R77H\Delta GFFKR}$ rescued its impaired catch-slip trend (Figures 3M and S4I–L). The resulting lifetime curve overlapped well with those of CBR LFA1/2-activated cells (Figure 3L). This suggests a central role for cytoplasmic tail separation in transmitting allosteric signals within the α-subunit for catch bond formation.

Another mutation, β_2^{V124A}, which stabilizes the βI domain in an active state that is more permissive for internal ligand binding (Sen et al., 2013), resulted in a higher effective 2D affinity in cells expressing α_M^{WT} (Figures 3E and S4D). β_2^{V124A} expression with α_M^{R77H} not only rescued the deficiency of α_M^{R77H} in the 2D affinity, but also increased it to be higher than $\alpha_M^{WT}\beta_2^{WT}$ (Figure 3E). The β_2^{V124A} had minor effects on the off-rate of α_M^{R77H} and α_M^{WT} (Figures 3F and S4D), indicating that the affinity increase resulted solely from the change in on-rate. Under force, V124A did not increase the peak lifetime of α_M^{R77H} (Figures 3N and S4M–P). However, the force regime of the “catch” phase was broadened to be similar to α_M^{WT}, indicating a partial rescue of the catch bond (Figure 3N). This partial rescue was not detected in the shear flow assay (Figure 2E), likely because off-rates and ligand densities also contribute to ligand-integrin interaction in this assay.

DISCUSSION

We demonstrate that the SLE associated Mac-1 variant R77H alters Mac-1’s 2D affinity and its ability to form catch-bonds, a counterintuitive strengthening of receptor–ligand bonds under mechanical forces. The latter provides a compelling explanation for the marked defect in this variant’s ability to bind ligand, primarily under flow conditions. Thus, R77H does not lead to an overall reduction in Mac-1 ligand binding. Rather, R77 plays a regulatory role, which is consistent with the fact that it is outside the ligand binding αI-domain. The rescue of the R77H bond lifetime under force with activating antibodies or mutations documented to induce allostery, identifies a specific role for R77 in force-induced Mac-1 bond stability, a finding that adds another level of complexity in the regulation of integrin function. Moreover, the phenocopy of R77H with β-propeller antibodies indicates new roles for R77, and the domain in which it resides in integrin allostery transmission, which is of interest, as the β-subunit has been primarily reported to transmit the conformational changes associated with ligand binding (Schurpf and Springer, 2011).

To explain the allosteric modulation of catch bonds by R77H, we propose a model based on the force balance within the integrin and the interplay of two catch bonds (Figure 4). The force balance is between the total force, F, applied to the αI domain by ICAM-1, and two component forces, F_α and F_β, supported by the integrin α and β subunits respectively (Figure 4C–H). F_α transmits through the αI domain N-terminus into the β-propeller domain near the lesion at R77 whereas F_β transmits through the αI domain α7 helix into the βI domain via the internal ligand (e.g. Figure 4C). The two catch bonds are 1) the external catch bond between the αI-domain and ligand elicited by the total F, and 2) the internal catch bond between the αI and βI domains via the internal ligand elicited by component force F_β. The two are coupled as the external catch bond requires pulling of αI domain α7 helix by the internal catch bond (Chen et al., 2010). The R77H mutation tilts the balance between the total force and the two component forces, resulting in a decrease in F_α and an increase in F_β (Figure 4C, D). This speeds up the increase of F_β with increasing F and results in an accelerated pulling of the αI-domain α7 helix by F_β at still small F. This manifests as an early rise of the Mac-1/ligand catch bond with longer lifetime for R77H than

WT at 5pN. A further increase in F (F>7pN) transitions the αI-βI interdomain interaction to a slip bond that is less able to pull on the αI-domain α7 helix to elicit the external catch bond with ligand, thus resulting in an earlier transition from the catch to slip bond regime for R77H compared to WT (Figure 4C,D). This explains the compression of the force range F of the Mac-1/ligand catch bond from 0–12pN for α_M^{WT} to 0–5pN for α_M^{R77H} (Figure 3K).

CBR LFA1/2 maximally activates Mac-1 by inducing full integrin extension. Separation of the α and β tails occurs upon binding of this antibody or deletion of the α-subunit GFFKR sequence, both of which augmented the catch-bond in α_M^{R77H} by force redistribution (Figure 4E,F). Mac-1 αI-domain exists in an equilibrium between closed/inactive and open/active states (Figure 4A–C) transiently coupling the binding of the external ligand to the binding of its internal ligand to the βI domain. A catch bond with ligand requires F_β to pull on the α7 helix to activate the αI-domain. We propose that cytoplasmic tail separation swings out the hybrid domain to activate the βI domain for binding of the internal ligand. The strengthened internal catch bond enables the allosteric relay between αI and βI domains and supports a higher F_β to amplify (for WT) and rescue (for R77H) the Mac-1/ligand catch bond (Figure 4E,F).

The V124A mutation stabilizes the βI domain in an active state that is more permissive for internal ligand binding (Sen et al., 2013). So the mechanism for the V124A mutation to broaden the force range of the αI-βI interdomain catch bond and to right-shift the lifetime versus force curve of the Mac-1/ligand catch bond may be qualitatively similar to, but quantitatively less effective than that of the CBR LFA1/2 and ΔGFFKR for both α_M^{WT} and α_M^{R77H} (Figure 4G,H). The suppressed Mac-1/ligand catch bond in R77H resembles, although less dramatically, the altered lifetime versus force curve of $\alpha_L\beta_2$'s bond with ICAM-1 in the presence of XVA143 (Chen et al., 2010), a small molecule antagonist that binds to the internal ligand binding site on the βI domain and blocks the conformation signal relay between the αI and βI subunits (Shimaoka et al., 2003). How R77H may structurally affect the αI and βI interdomain communication required for catch bonds requires further study.

The R77H variant is a common allele in the healthy population (~10%). In non-autoimmune conditions, the influence of this variant may be minor, due to the existence of many regulatory checkpoints. However, in SLE, where dysfunction of several aspects of the immune response occurs simultaneously, the R77H variant might impact disease. The possibility that R77H, in linkage disequilibrium with a true causative mutation is responsible for the observed phenotypes is unlikely as the defects observed in neutrophils expressing R77H as well as other SNPs, was similar to that in a cell line expressing R77H alone. How would compromised Mac-1 2D affinity for ligand and catch bond formation, as observed in the R77H variant, increase SLE susceptibility? In addition to its pro-inflammatory roles, Mac-1 has immunosuppressive functions and inhibits the signaling of immune cell receptors (Fagerholm et al., 2013) implicated in SLE pathogenesis (Tsokos, 2011). Although the precise mechanisms through which Mac-1 exerts its down-modulatory effects remain to be determined, a developing concept in other systems is that monomeric ligation of a receptor leads to inhibitory signaling, while multivalent ligation promotes activating signals (Blank et al., 2009; Ivashkiv, 2011). Thus, we propose that a reduction in Mac-1 2D ligand affinity in the absence of high valency ligand, may prevent Mac-1's inhibitory function. For the same argument, impaired stability of single receptor/ligand bonds under mechanical force (catch bonds), in the absence of multivalent Mac-1 ligand engagement, may compromise inhibitory Mac-1 signaling. Mac-1 upregulation of FcγR functions is well known (Jones and Brown, 1996), but in models of lupus, an autoimmune disease characterized by high levels of immune complexes (Tsokos, 2011), Mac-1 deficiency leads to a significant increase in glomerular neutrophil accumulation and lupus nephritis (Kevil et al., 2004; Rosetti et al., 2012). The IgG/immune complex receptor FcγRIIA, mediates neutrophil adhesion to intravascular deposited soluble IgG-immune complexes (Tsuboi et al., 2008) that is enhanced by Mac-1 deficiency (Rosetti et al., 2012). During FcγRIIA mediated neutrophil interactions with intravascular immune complexes, a defect in bond stability between Mac-1 R77H and ligand upon force exerted by blood flow, could impact Mac-1's downregulatory function on FcγRIIA and thus augment neutrophil accumulation.

Allosteric catch bonds have been reported for several hematopoietic cell receptor/ligand pairs. Our data showing that a Mac-1 variant that confers high risk for developing lupus alters the relay of allosteric signals required for catch bonds, suggests that elimination of catch bonds may have pathological consequences.

EXPERIMENTAL PROCEDURES

Human neutrophils, lentiviral constructs and generation of K562 cell lines

Genotyped human blood samples from non- or risk variant (R77H)-carrying donors were provided by the Genotype and Phenotype Registry, a service of the Tissue Donation Program at The Feinstein Institute for Medical Research, Manhasset, NY, USA. β-propeller antibodies were used on neutrophils from blood of healthy volunteers under approved protocols (Brigham and Women's Hospital IRB). R77H and the GFFKR mutant, generated by including a stop codon before the GFFKR sequence, were generated in human α_M by PCR. β_2^{V124A} and β_2^{L132A} cDNA constructs were as described (Sen et al., 2013). All constructs were cloned into lentiviral plasmids (see Supplemental Information). K562 cells, which lack endogenous α_M and β_2, were transduced with lentiviruses and sorted for positive expressing cells. Multiple clones expressing similar surface levels of Mac-1 were used in functional assays.

Static and shear flow adhesion assays

Integrin Activation—For Mg^{2+}/EGTA induced activation, K652 cells were washed with HBSS without Ca^{2+} and Mg^{2+} (Lonza) with 5mM EDTA, washed again with HBSS and resuspended in HBSS plus Mg^{2+}/EGTA (2mM of each). For Mn^{2+} induced activation, K562 cells were washed in HEPES plus 2mM EGTA and 0.5mM $MnCl_2$, and resuspended in HEPES/1mM $MnCl_2$. Neutrophils were activated with 500nM fMLP in PBS plus 2mM Ca^{2+} and Mg^{2+}.

Details on ligand coating are in Supplemental Information

Static adhesion assays—Cells were labeled with CFSE (Molecular Probes, Invitrogen), and placed on ligand-coated surfaces plus activating stimuli and the percentage of adherent cells relative to α_M^{WT} cells treated with Mn^{2+} was calculated. For blocking experiments using the anti- β-propeller antibodies, the percent inhibition relative to CBR LFA1/7 control was calculated.

Shear flow adhesion assay—Cells were perfused through a flow chamber at 1 dynes/cm^2 for a min. Shear flow was then decreased to 0.19–0.67 dynes/cm^2, and the number of cells accumulating in four different fields after two minutes was calculated. Further details are in Supplemental Information.

Spreading and crawling assay—Details are in Supplemental Information.

Biomembrane Force Probe (BFP)—The details of BFP have been previously described (Chen et al., 2008b). Details of RBC and bead preparation and BFP analysis are in Supplemental Information.

Adhesion frequency assay—An adhesion frequency assay reports the 2D binding kinetics between the receptor and ligand, details of which are in Supplemental Information.

Thermal fluctuation assay—Thermal fluctuation assay was used for lifetime measurements under zero-force (Chen et al., 2008a; Chen et al., 2010). The ICAM-1 coating densities of the beads were adjusted to achieve ≤20% adhesion frequency as required for single-bond adhesion events. Details are in Supplemental Information.

Force-clamp assay—The previously described force-clamp assay was used to measure bond lifetimes under a constant force (Chen et al., 2010). Details are in Supplemental Information.

Lifetime analysis—Lifetimes were categorized into bins of successive force ranges, each of which has an approximate width of 5pN. The average lifetime in each force bin was collected to plot the lifetime curve as a function of clamping force.

Statistical analysis

All data are Mean ± SEM. Statistical significance of the differences was determined by Student *t*-test. For group analysis, two-way ANOVA was used. If significant differences were shown, data was subjected to Tukey test for multiple comparisons. $P<0.05$ was considered significant.

Supplementary Material

Refer to Web version on PubMed Central for supplementary material.

ACKNOWLEDGEMENTS

This work was supported by, the NIH HL065095 (to TM) and AI044902 (to CZ); Target Identification in Lupus Grant/Alliance for Lupus Research Foundation (to TM); Consejo Nacional de Ciencia y Tecnologia and Fundación México en Harvard (to FR); T32 HL007627 (to FR); German Research Foundation HE-6810/1-1 (to JH). We thank Dr. T. Springer (Boston, MA) for providing β_2 antibodies.

REFERENCES

Abram CL, Lowell CA. Leukocyte adhesion deficiency syndrome: a controversy solved. Immunology and Cell Biology. 2009; 87:440–442. [PubMed: 19417769]

Blank U, Launay P, Benhamou M, Monteiro RC. Inhibitory ITAMs as novel regulators of immunity. Immunological Reviews. 2009; 232:59–71. [PubMed: 19909356]

Carman CV, Springer TA. Integrin avidity regulation: are changes in affinity and conformation underemphasized? Current Opinion in Cell Biology. 2003; 15:547–556. [PubMed: 14519389]

Chen W, Evans EA, McEver RP, Zhu C. Monitoring receptor-ligand interactions between surfaces by thermal fluctuations. Biophysical Journal. 2008a; 94:694–701. [PubMed: 17890399]

Chen W, Lou J, Zhu C. Forcing switch from short- to intermediate- and long-lived states of the alphaA domain generates LFA-1/ICAM-1 catch bonds. The Journal of Biological Chemistry. 2010; 285:35967–35978. [PubMed: 20819952]

Chen W, Zarnitsyna VI, Sarangapani KK, Huang J, Zhu C. Measuring Receptor-Ligand Binding Kinetics on Cell Surfaces: From Adhesion Frequency to Thermal Fluctuation Methods. Cellular and Molecular Bioengineering. 2008b; 1:276–288. [PubMed: 19890486]

Chesla SE, Selvaraj P, Zhu C. Measuring two-dimensional receptor-ligand binding kinetics by micropipette. Biophysical Journal. 1998; 75:1553–1572. [PubMed: 9726957]

Choi YI, Duke-Cohan JS, Chen W, Liu B, Rossy J, Tabarin T, Ju L, Gui J, Gaus K, Zhu C, et al. Dynamic control of beta1 integrin adhesion by the plexinD1-sema3E axis. Proceedings of the National Academy of Sciences USA. 2014; 111:379–384.

Evans E, Ritchie K, Merkel R. Sensitive force technique to probe molecular adhesion and structural linkages at biological interfaces. Biophysical Journal. 1995; 68:2580–2587. [PubMed: 7647261]

Fagerholm SC, MacPherson M, James MJ, Sevier-Guy C, Lau CS. The CD11b-integrin (ITGAM) and systemic lupus erythematosus. Lupus. 2013; 22:657–663. [PubMed: 23753600]

Faridi MH, Altintas MM, Gomez C, Duque JC, Vazquez-Padron RI, Gupta V. Small molecule agonists of integrin CD11b/CD18 do not induce global conformational changes and are significantly better than activating antibodies in reducing vascular injury. Biochimica et Biophysica Acta. 2013; 1830:3696–3710. [PubMed: 23454649]

Fiore VF, Ju L, Chen Y, Zhu C, Barker TH. Dynamic catch of a Thy-1-α5β1+syndecan-4 trimolecular complex. Nature Communication. 2014; 5:4886.

Han S, Kim-Howard X, Deshmukh H, Kamatani Y, Viswanathan P, Guthridge JM, Thomas K, Kaufman KM, Ojwang J, Rojas-Villarraga A, et al. Evaluation of imputation-based association in and around the integrin-alpha-M (ITGAM) gene and replication of robust association between a non-synonymous functional variant within ITGAM and systemic lupus erythematosus (SLE). Human Molecular Genetics. 2009; 18:1171–1180. [PubMed: 19129174]

Hom G, Graham RR, Modrek B, Taylor KE, Ortmann W, Garnier S, Lee AT, Chung SA, Ferreira RC, Pant PV, et al. Association of systemic lupus erythematosus with C8orf13-BLK and ITGAM-ITGAX. The New England Journal of Medicine. 2008; 358:900–909. [PubMed: 18204098]

Ivashkiv LB. How ITAMs inhibit signaling. Science Signaling. 2011; 4:pe20. [PubMed: 21505184]

Jones, SLB, Brown, EJ. Functional cooperation between Fcg receptors and complement receptors in phagocytes. In: van de Winkel, JGC, Capel, PJA, editors. Human IgG Fc receptors. Austin, TX: USA: R.G. Landes Co.; 1996. 149–163.

Kanse SM, Matz RL, Preissner KT, Peter K. Promotion of leukocyte adhesion by a novel interaction between vitronectin and the beta2 integrin Mac-1 (alphaMbeta2, CD11b/CD18). Arteriosclerosis, Thrombosis, and Vascular Biology. 2004; 24:2251–2256.

Kevil CG, Hicks MJ, He X, Zhang J, Ballantyne CM, Raman C, Schoeb TR, Bullard DC. Loss of LFA-1, but not Mac-1, protects MRL/MpJ-Fas(lpr) mice from autoimmune disease. The American Journal of Pathology. 2004; 165:609–616. [PubMed: 15277234]

Kim M, Carman CV, Springer TA. Bidirectional transmembrane signaling by cytoplasmic domain separation in integrins. Science. 2003; 301:1720–1725. [PubMed: 14500982]

Kong F, Garcia AJ, Mould AP, Humphries MJ, Zhu C. Demonstration of catch bonds between an integrin and its ligand. The Journal of Cell Biology. 2009; 185:1275–1284. [PubMed: 19564406]

Lefort CT, Hyun YM, Schultz JB, Law FY, Waugh RE, Knauf PA, Kim M. Outside-in signal transmission by conformational changes in integrin Mac-1. Journal of Immunology. 2009; 183:6460–6468.

Lu CF, Springer TA. The alpha subunit cytoplasmic domain regulates the assembly and adhesiveness of integrin lymphocyte function-associated antigen-1. Journal of Immunology. 1997; 159:268–278.

Lu C, Ferzly M, Takagi J, Springer TA. Epitope mapping of antibodies to the C-terminal region of the integrin beta 2 subunit reveals regions that become exposed upon receptor activation. J. Immunol. 2001; 166:5629–5637. [PubMed: 11313403]

O'Brien XM, Heflin KE, Lavigne LM, Yu K, Kim M, Salomon AR, Reichner JS. Lectin site ligation of CR3 induces conformational changes and signaling. The Journal of Biological Chemistry. 2012; 287:3337–3348. [PubMed: 22158618]

Petruzzelli L, Maduzia L, Springer TA. Activation of lymphocyte functionassociated molecule-1 (CD11a/CD18) and Mac-1 (CD11b/CD18) mimicked by an antibody directed against CD18. Journal of immunology. 1995; 155:854–866.

Phillipson M, Heit B, Colarusso P, Liu L, Ballantyne CM, Kubes P. Intraluminal crawling of neutrophils to emigration sites: a molecularly distinct process from adhesion in the recruitment cascade. The Journal of Experimental Medicine. 2006; 203:2569–2575. [PubMed: 17116736]

Rosetti F, Tsuboi N, Chen K, Nishi H, Ernandez T, Sethi S, Croce K, Stavrakis G, Alcocer-Varela J, Gomez-Martin D, et al. Human lupus serum induces neutrophilmediated organ damage in mice that is enabled by Mac-1 deficiency. Journal of Immunology. 2012; 189:3714–3723.

Schurpf T, Springer TA. Regulation of integrin affinity on cell surfaces. The EMBO Journal. 2011; 30:4712–4727. [PubMed: 21946563]

Sen M, Yuki K, Springer TA. An internal ligand-bound, metastable state of a leukocyte integrin, alphaXbeta2. The Journal of Cell Biology. 2013; 203:629–642. [PubMed: 24385486]

Shimaoka M, Salas A, Yang W, Weitz-Schmidt G, Springer TA. Small molecule integrin antagonists that bind to the beta2 subunit I-like domain and activate signals in one direction and block them in the other. Immunity. 2003; 19:391–402. [PubMed: 14499114]

Sokurenko EV, Vogel V, Thomas WE. Catch-bond mechanism of force-enhanced adhesion: counterintuitive, elusive, but … widespread? Cell Host & Microbe. 2008; 4:314–323. [PubMed: 18854236]

Tsokos GC. Systemic lupus erythematosus. The New England Journal of Medicine. 2011; 365:2110–2121. [PubMed: 22129255]

Tsuboi N, Asano K, Lauterbach M, Mayadas TN. Human neutrophil Fcgamma receptors initiate and play specialized nonredundant roles in antibody-mediated inflammatory diseases. Immunity. 2008; 28:833–846. [PubMed: 18538590]

Xiang X, Lee CY, Li T, Chen W, Lou J, Zhu C. Structural basis and kinetics of force-induced conformational changes of an alphaA domain-containing integrin. PloS One. 2011; 6:e27946. [PubMed: 22140490]

Xiao T, Takagi J, Coller BS, Wang JH, Springer TA. Structural basis for allostery in integrins and binding to fibrinogen-mimetic therapeutics. Nature. 2004; 432:59–67. [PubMed: 15378069]

Xiong JP, Stehle T, Goodman SL, Arnaout MA. Integrins, cations and ligands: making the connection. Journal of Thrombosis and Haemostasis. 2003; 1:1642–1654. [PubMed: 12871301]

Yalamanchili P, Lu C, Oxvig C, Springer TA. Folding and function of I domain-deleted Mac-1 and lymphocyte function-associated antigen-1. The Journal of Biological Chemistry. 2000; 275:21877–21882. [PubMed: 10764808]

Yu Y, Zhu J, Mi LZ, Walz T, Sun H, Chen J, Springer TA. Structural specializations of alpha(4)beta(7), an integrin that mediates rolling adhesion. The Journal of Cell Biology. 2012; 196:131–146. [PubMed: 22232704]

Zhou Y, Wu J, Kucik DF, White NB, Redden DT, Szalai AJ, Bullard DC, Edberg JC. Multiple lupus-associated ITGAM variants alter Mac-1 functions on neutrophils. Arthritis and Rheumatism. 2013; 65:2907–2916. [PubMed: 23918739]

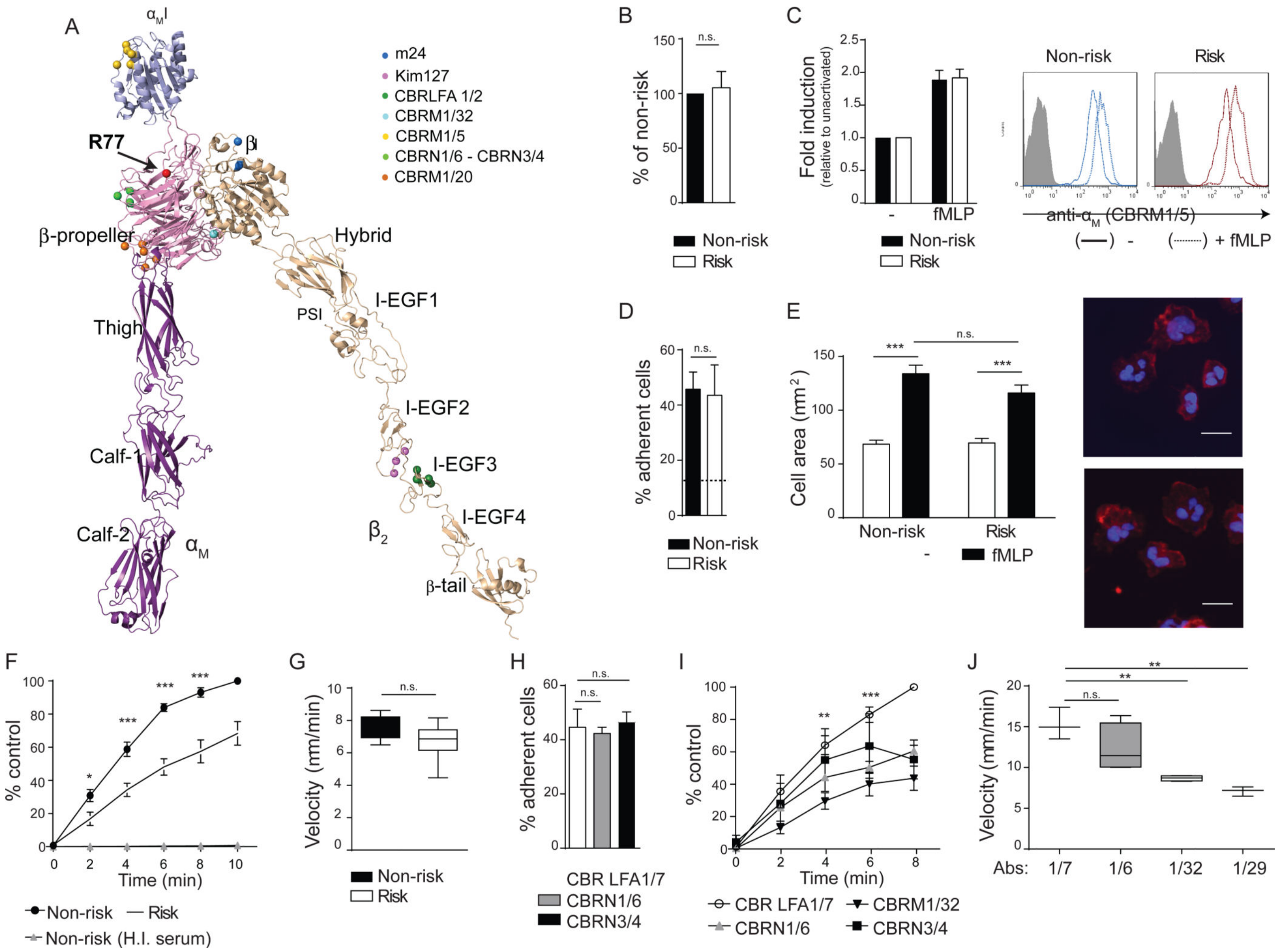

Figure 1. Functional effects of the *ITGAM* R77H risk variant in human neutrophils

(A) Model of $\alpha_M\beta_2$ ectodomains. The R77 region (arrow) and epitopes for antibodies are indicated. **(A–G)** Neutrophils from non- and risk- variant donors were treated with fMLP or vehicle control(−). Surface expression of α^M **(B)** and CBRM1/5 antibody binding **(C)** was examined by flow cytometry. Data is fold induction relative to vehicle treated cells. Representative histograms are shown. **(D)** Adhesion of neutrophils to an iC3b-coated surface under static conditions. Dotted line is binding of cells to a surface with heat-inactivated serum (H.I.). n=4 experiments. **(E)** Spreading of neutrophils on iC3b. Cell area was quantified, and representative photographs of cells stained with phalloidin (red) and DAPI (blue) are shown. Scale bar=10μm. **(F)** Adhesion of neutrophils to iC3b under shear flow (0.38dynes/cm^2) at the indicated time points. Results are percent of adherent neutrophils relative to the non-risk donor at 10 min. n=7–8 per genotype. **(G)** Crawling velocity of neutrophils over a plasma-coated surface. n=4 per genotype. **(H–J)** Neutrophils from healthy volunteers were treated with CBRN1/6, CBRN 3/4 or CBRM1/32 antibodies to block specific β-propeller regions, CBRM1/29 to block the αI-domain or CBR LFA1/7, a non-blocking antibody binding control. Cell adhesion under static **(H)** and shear flow **(I)** conditions, and crawling velocity **(J)** were evaluated. n.s, no statistical significance, *p<0.05, **p<0.01, ***p<0.001 between neutrophils from non- and risk variant, and neutrophils with non-blocking versus blocking antibodies. See also Figure S1 and Table S1.

Author Manuscript
Author Manuscript
Author Manuscript

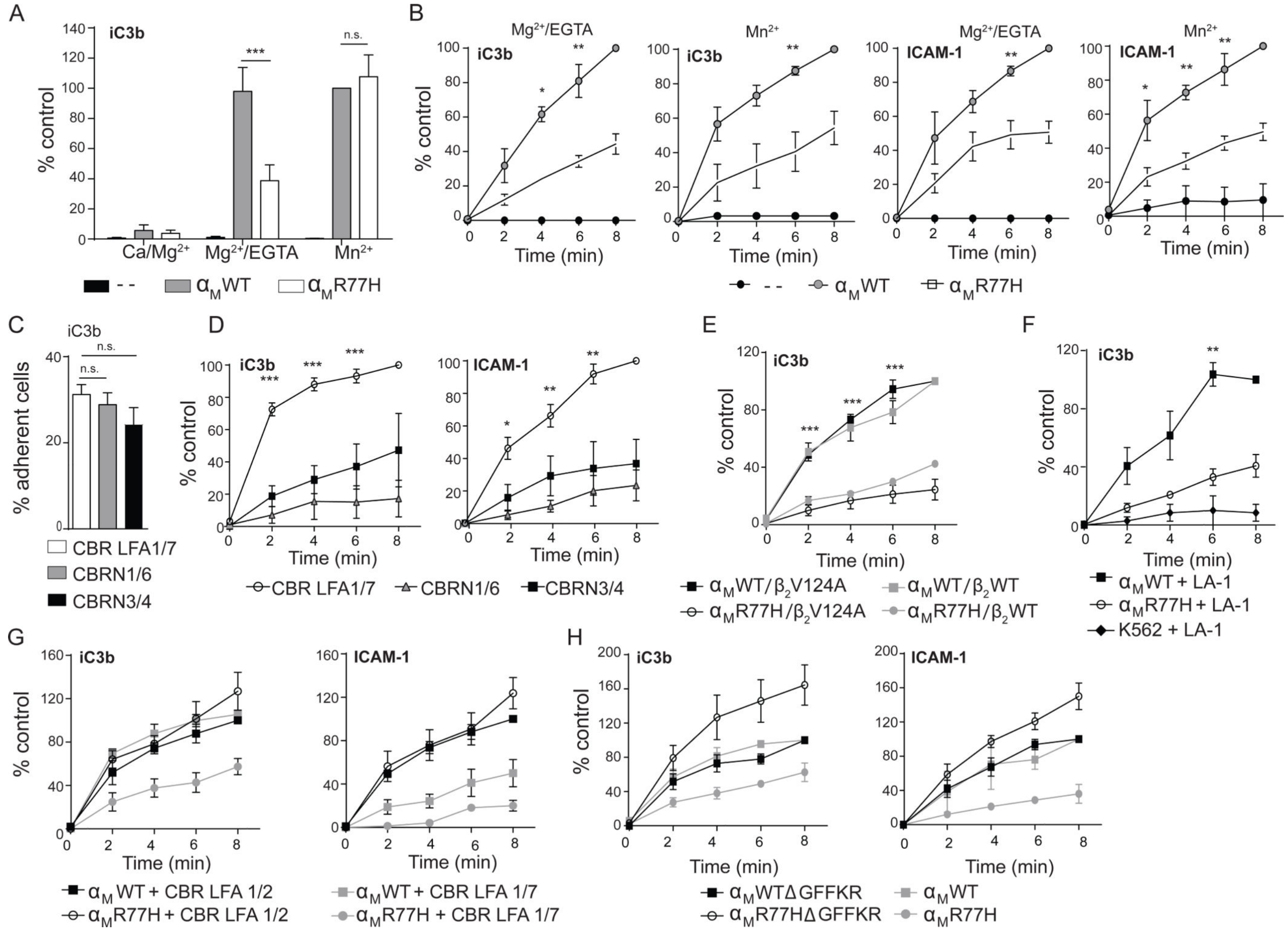

Figure 2. Functional effects of R77H in K562 cells

K562 cells lacking β_2 integrins (--), or stably expressing α_M^{WT} or α_M^{R77H} with β_2 were evaluated for adhesion to iC3b and ICAM-1 following activation with Mn^{2+} or Mg^{2+}/EGTA, under static conditions or flow conditions. **(A)** Adhesion of α_M^{WT} or α_M^{R77H} cells to iC3b-coated surfaces under static conditions. Results are presented as percent of adherent cells relative to cells expressing α_M^{WT} plus Mn^{2+}. n=6 experiments. **(B)** Adhesion of α_M^{WT} or α_M^{R77H} cells to iC3b and ICAM-1 under shear flow (0.38 dynes/cm^2) evaluated at the indicated time points. Results are presented as percent of adherent cells relative to cells expressing α_M^{WT} at 8min. n=3–4 independent experiments. **(C–D)** Binding of α_M^{WT}- cells to ligand-coated surfaces following treatment with indicated β-propeller antibodies (as in Figure 1) under static **(C)** or shear flow **(D)** conditions. **(E)** Cell adhesion under shear flow in cells expressing α_M^{WT} or α_M^{R77H} with β_2^{WT} or β_2^{V124A}. **(F–G)** Adhesion of α_M^{WT} or α_M^{R77H} cells pretreated with leukoadherin-1 (LA-1) or vehicle control **(F)** or CBR LFA1/2 or control antibody, CBR LFA1/7 **(G)**. **(H)** Adhesion of cells expressing α_M^{WT} or α_M^{R77H} with or without a GFFKR deletion (Δ). n=3 for panels E–H. **p<0.01, ***p<0.001. See also Figure S2, S3 and Table S1.

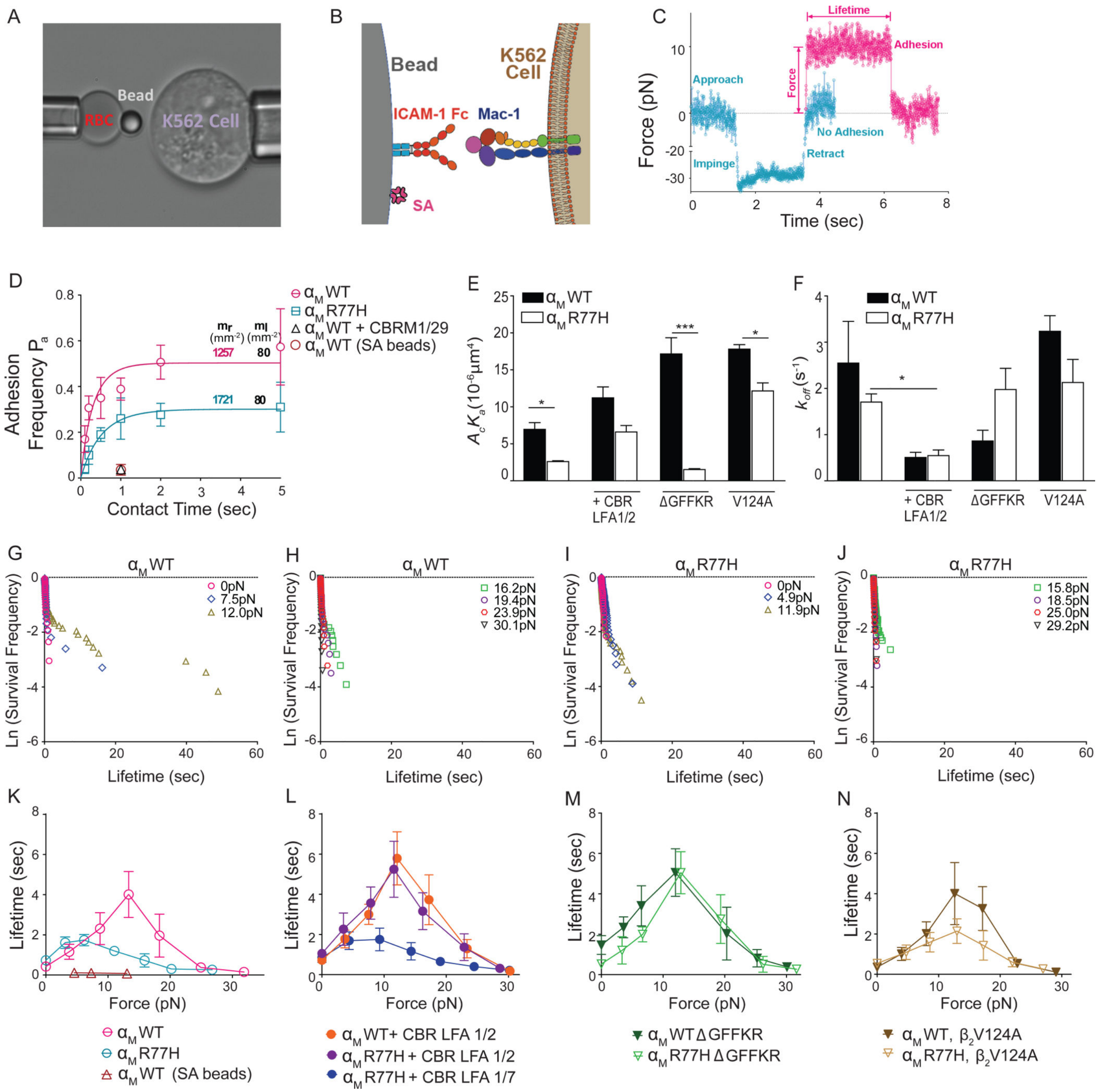

Figure 3. Characterization of Mac-1/ICAM-1 binding kinetics and catch bond formation by a biomembrane force probe

(A) A micrograph of a BFP experiment is shown. A micropipette-aspirated RBC with an ICAM-1-coated probe bead attached to the apex (left) via biotin-streptavidin interaction was aligned against a target Mac-1-expressing K562 cell held by an opposing micropipette (right). **(B)** A sketch of the probe-bead double covalently coated with recombinant ICAM-1 and streptavidin and the K562 cell expressing Mac-1. **(C)** Superposition of force-traces of two BFP contact cycles without (cyan) and with (magenta) an adhesion event. Without binding the retraction curve returns to zero force upon target cell retraction. A contact cycle with adhesion, held at 10pN, renders a lifetime until dissociation. **(D)** Adhesion frequency versus contact time plot of the indicated cell lines. Site densities of Mac-1 (m_r) and ICAM-1 (m_l, 80μm^{-2}) are marked along each curve. Binding frequency of α_M^{WT}/ICAM-1 with either CBRM1/29 antibody (open black triangle), or streptavidin coated beads (SA) (open brown circle) at 1-s contact are shown. **(E, F)** Effective 2D affinity (A_cK_a, **E**) and off-rate (k_{off}, **F**) of each Mac-1/ICAM-1 pair calculated from fitting Eqn 1 (in Methods) to the adhesion frequency data. **(G–J)** Semi-log survival frequency versus bond lifetime plots of α_M^{WT} (**G, H**) and α_M^{R77H} (**I, J**) cells dissociating from the ICAM-1 bead under 0–12pN (**G**, **I**) or >12pN (**H, J**) forces. Survival frequency is calculated as the fraction of the binding events with a lifetime longer than a certain value t (sec). **(K–N)** Plots of mean ± SEM bond lifetime versus force of α_M^{WT} and α_M^{R77H} cells dissociating from ICAM-1 beads in the absence **(K)** or presence **(L)** of CBR LFA1/2 or CBR LFA1/7 control antibody, or with a GFFKR deletion **(M)** or a $\beta^{2\ V124}$ mutation **(N)**. See also Figure S4.

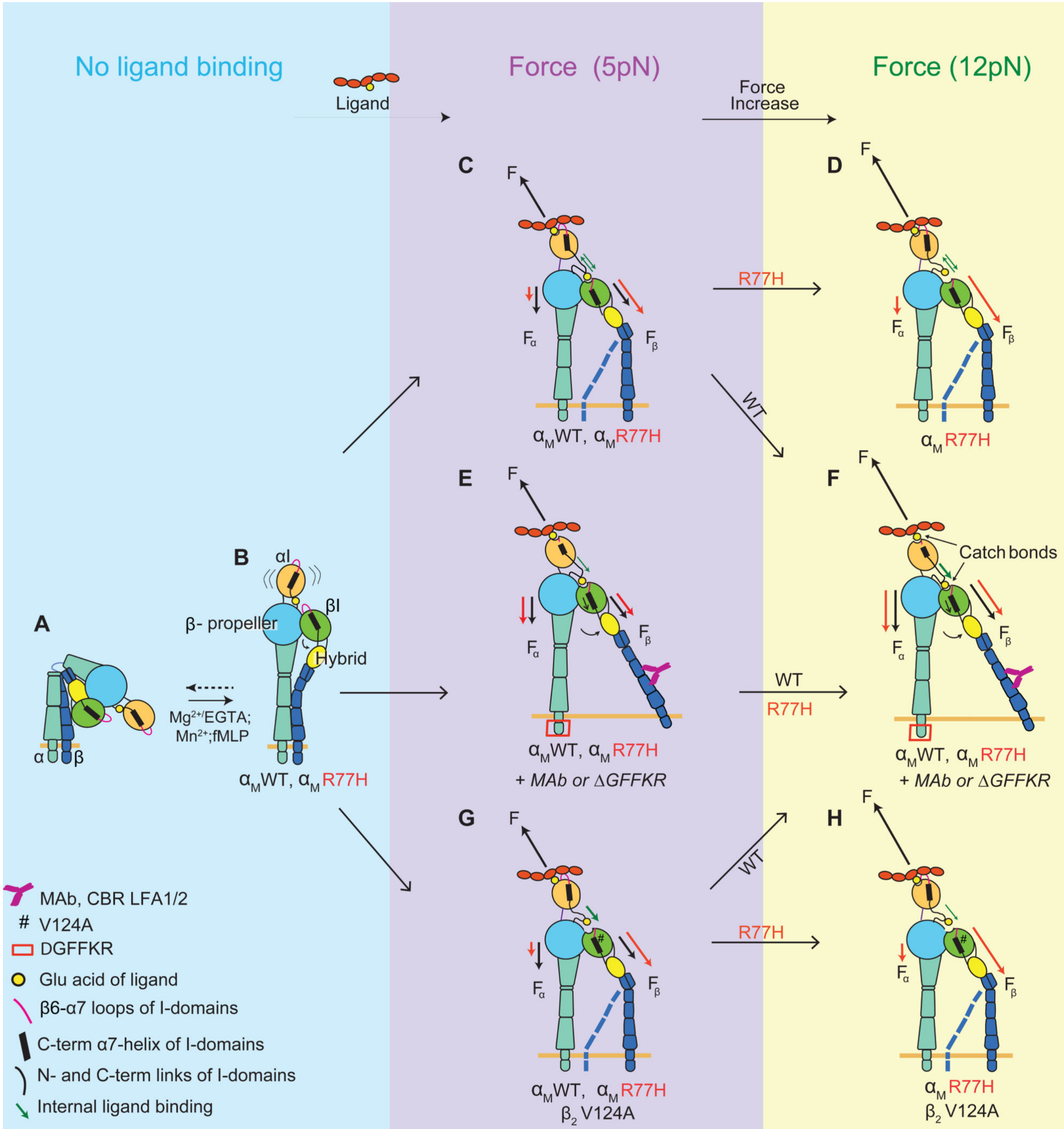

Figure 4. Model on how R77H affects ligand binding and catch bond formation by Mac-1

(A) Inactive, bent Mac-1 with a closed headpiece. The αI-domain is in the inactive conformation with the α7-helix in the up position and the MIDAS in the closed conformation. **(B)** Mac-1 extension induced by inside-out signaling (fMLP) or activating metal ions. **(C–H)** Mac-1 under a lower (5pN) **(C, E and G)** or a higher (12pN) **(D, F and H)** stretching force following ligand binding is shown. The blue dotted line for CD18 in **C, D, G and H** depicts the cytoplasmic tail in a clasped (like **B**) or unclasped position. Force (*F*) applied by the ligand and the component forces from the αI-domain MIDAS to the β-propeller (F_α) or the βI (F_β) domain are black for WT and red for R77H. R77H perturbs the force distribution so that more force is transmitted to the βI domain and induces a premature catch bond at lower force **(C)**, while at the higher force F_β exceeds the optimal value for αI- and βI-domain interaction and results in a weaker binding capacity **(D)**. Forced ectodomain extension and tail separation by CBR LFA1/2 antibody or deletion of the regulatory GFFKR of the α subunit restores the force redistribution in R77H and hence rescues R77H by swinging out the hybrid domain to activate the βI-domain and strengthen the αI-βI interdomain catch bond to prolong bond lifetime **(E and F)**. The V124A mutation (#) moves the βI-domain into a more activated state and therefore more stable internal ligand binding (green arrow), which partially rescues the R77H catch bond defect **(H)** but to a lesser extent and hence does not fix the perturbed force distribution in R77H **(G)**.